

DISCOVERY OF ALUNITE IN CANDIDATE EXOMARS LANDING SITE, MAWRTH VALLIS: EVIDENCE FOR LOCALIZED EVAPORATIVE ENVIRONMENTS. A. M. Sessa¹, J. J. Wray¹, and J. L. Bishop², ¹Georgia Institute of Technology, Atlanta, GA (asessa3@gatech.edu), ²SETI Institute, Mountain View, CA

Introduction: The spatially expansive, phyllosilicate-rich terrain of Mawrth Vallis was first observed using the OMEGA (Observatoire pour la Mineralogie, l'Eau, les Glaces et l'Activité) instrument aboard Mars Express [1][2]. On a broad scale, these layered light-toned deposits (of sedimentary and/or pyroclastic origin) [3][4] that constitute this altered early to middle Noachian-aged terrain (i.e., >3.7 Ga) [5] are spectrally consistent with stratified Al- and Fe/Mg-phyllsilicates (i.e., Al-smectites/kaolins overlying Fe/Mg-smectites) [6-9]. Locally, occurrences of sulfates, and other products of acidic leaching, have been reported throughout the region [10-13].

Notably absent, however, is the Al-rich sulfate Alunite, which has been observed in Columbus and Cross craters (as well as, a small light-toned deposit within the intercrater plateau) in the Terra Sirenum region of the Martian southern highlands [14-17]. These craters exhibit a particular suite of minerals (i.e., kaolins, hydrated silica, “doublet” phase, and sulfates) that indicate upwelling acidic (+/- sulfate-rich) groundwater had previously fed closed-basin lakes [18], which in turn lead to the subsequent formation of evaporite deposits. Indeed, it has been proposed that isolated (or closed-system) ponds, with similar water chemistries as the aforementioned crater lake environments, are responsible for the observed sulfate-rich outcrops in Mawrth Vallis [19]. Other possible formation mechanisms (e.g., magmatic hydrothermal systems, supergene alteration, and highly acidified snows/rains) are discussed in [17].

In particular, the precipitation of Al-rich phases (i.e., kaolins and alunite) is favored as pH decreases, thereby increasing the solubility of Al^{3+} and mobilizing it in solution, with alunite forming at lower pH and/or higher sulfate activity than kaolinite. Aluminum must also be many times more concentrated than iron for alunite to preferentially form over other sulfates [17].

Interestingly, Mawrth Vallis, Cross, and Columbus craters occur in early Noachian terrain, which has been shown to have a detectable feldspar component [20]. A more felsic precursor, coupled with acid alteration, could potentially play an accessory role in the formation of alunite on Mars.

Methods: Compact Reconnaissance Imaging Spectrometer for Mars (CRISM) observations, that could be contained within the potential ExoMars landing ellipse for Mawrth Vallis, were analyzed in search of alunite and additional exposures of Fe- (e.g., jarosite) and Ca-sulfates (e.g., gypsum and bassanite) that have been identified in the western portion of the landing ellipse and elsewhere in the region (e.g., [10][21]). Here, we focus primarily on full resolution targeted observations

(i.e., 18 m/pixel), FRT0000C467 and FRT00003BFB. The revised summary parameters by [22] were utilized to detect spectral features that are unique to these phases (e.g., BD1750, BD2265, and BD2500). We focus primarily on the distribution of alunite and its relationship to Al/Fe/Mg-phyllsilicates here, as other studies have presented new observations consistent with the presence of additional jarosite and Ca-sulfate exposures [19][23]. A custom red-green-blue (RGB) color composite “browse product” was utilized to best visualize the distribution of alunite relative to other Al-bearing phases (BD2190) and Fe/Mg-phyllsilicates (D2300) (Fig. 2).

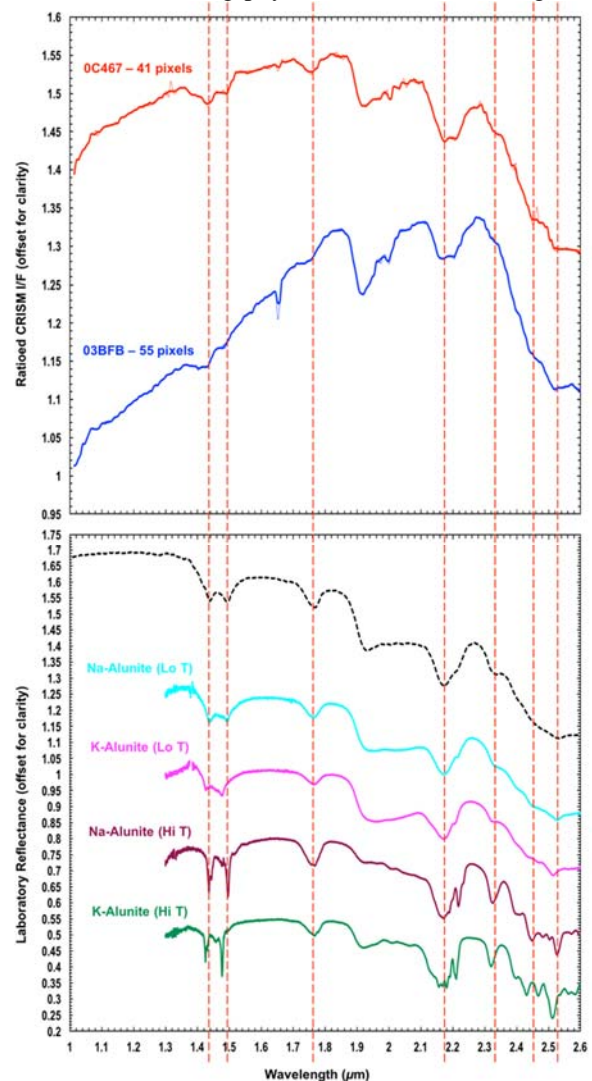


Figure 1. CRISM spectra from small, alunite-bearing outcrops in Mawrth Vallis (top) and USGS laboratory spectra of alunite (bottom). Low-temperature (150°C) Na-alunite is sample GDS95, high-temperature (450°C) Na-alunite is RES-3, low-T K-alunite is GDS97, high-T K-alunite is RES-2. Colored

spectra are synthetically derived, while the black dotted line spectrum is sourced from a low-temperature, lacustrine environment and of the Na-variety (GDS82). All spectra are from [31]. Red dashed lines indicate characteristic absorptions of Na-bearing, low-temperature (and high-temperature) alunite.

Alunite is distinguished by a strong, broad absorption centered at $2.17 \mu\text{m}$, with additional bands at $1.43\text{--}1.44$, $1.47\text{--}1.49$, 1.76 , 2.32 , and $2.51\text{--}2.53 \mu\text{m}$ (those with a range of values are at longer wavelengths in Na-end-member than in K-bearing alunite) [24][25]. On Mars, alunite is usually mixed with other Al-bearing mineral phases (i.e., allophane [26], kaolins [27], and smectites [e.g., 28]) with spectral features in a similar wavelength range (i.e., $2.16\text{--}2.21 \mu\text{m}$), making it difficult to identify unless it is the spectrally dominant phase.

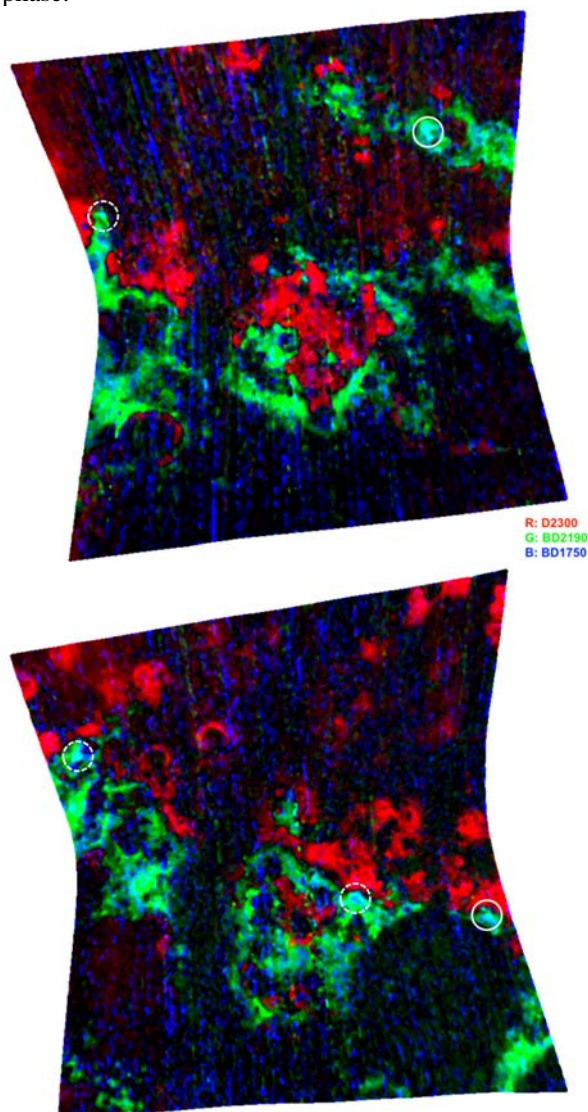


Figure 2. Browse products derived from CRISM observations FRT0000C467 (top) and FRT00003BFB (bottom) highlighting the distribution of Fe/Mg-smectite (red), kaolins (green), and alunite +/- kaolins (cyan). The white circled regions correspond to the red (0C467) and blue spectra (03BFB) in Fig.

1, while the white dashed circles indicate probable alunite-bearing material.

Spectral ratios are employed to accentuate the absorption features emanating from surface materials of interest and minimize atmospheric and instrumental contributions.

Results: We have identified two sites within our region of study that are spectrally consistent with an alunite/kaolin mixture (e.g., red and blue spectra in Fig. 1), as well as four probable detections that are highlighted in Fig. 2. As alunite/kaolinite do not typically display a pronounced hydration band at $\sim 1.92 \mu\text{m}$, another phase must be responsible for this feature (e.g., halloysite and/or hydrated silica). When compared to the USGS spectral library, the alunite spectra presented here is most similar to that formed in low-temperature terrestrial environments (e.g., lake/pond-like settings, like those in SW Australia [29][30]) and produced synthetically at lower temperatures (cyan and magenta spectra in Fig. 1). Here, we can rule out the possibility of a hydrothermal genesis for the Mawrth Vallis alunite based solely on spectral evidence, as alunite produced at higher temperatures are distinctly different (i.e., sharper features at 1.44 , 1.49 , 2.32 , 2.45 , and $2.52 \mu\text{m}$). Compositionally, the alunite observed in both CRISM scenes appears to be Na-bearing (versus K-bearing), based on the longer wavelength position of bands in the $1.47\text{--}1.49$ and $2.51\text{--}2.53 \mu\text{m}$ regions.

Summary: The rare mineral phase alunite has been detected in a third locality on the Martian surface and is likely to have formed in a low-temperature, acid-saline, evaporative lacustrine environment, possibly from a compositionally distinct precursor.

References: [1] Poulet F. et al. (2005) *Nature*, 438, 623–627. [2] Bibring J. P. et al. (2006) *Science*, 312, 400–404. [3] Loizeau D. et al. (2007) *JGR: Planets*, 112, E08S08. [4] Michalski J. R. and Noe Dobraea E. Z. (2007) *Geology*, 35, 951–954. [5] Loizeau D. et al. (2012) *PSS*, 72, 31–43. [6] Wray J. J. (2008) *GRL*, 35, L12202. [7] Bishop J. L. et al. (2008) *Science*, 321, 830–833. [8] McKeown N. K. et al. (2009) *JGR: Planets*, 114, E00D10. [9] Loizeau D. et al. (2010) *Icarus*, 205, 396–418. [10] Farrand W. H. et al. (2009) *Icarus*, 204, 478–488. [11] Farrand W. H. et al. (2014) *Icarus*, 241, 346–357. [12] Noe Dobraea E. Z. et al. (2011) *IJMSE*, 6, 32–46. [13] Michalski J. R. et al. (2013) *Icarus*, 226, 816–840. [14] Swayze G. A. et al. (2006) *Martian Sulfates as Recorders of Atmospheric-Fluid-Rock Interactions*, Abstract #7072. [15] Swayze G. A. et al. (2008) *AGU Fall Meeting*, Abstract #P44A-04. [16] Wray J. J. et al. (2011) *JGR: Planets*, 116, E01001. [17] Ehlmann B. L. et al. (2016) *Am. Mineral.*, 101, 1527–1542. [18] Goudge T. A. et al. (2015) *Icarus*, 260, 346–367. [19] Bishop J. L. et al. (2018) *LPS XLIX*, Abstract #1117. [20] Sessa A. M. and Wray J. J. (2017) *AGU Fall Meeting*, Abstract #P33B-2881. [21] Wray J. J. et al. (2010) *Icarus*, 209, 416–421. [22] Viviano-Beck C. E. et al. (2014) *JGR: Planets*, 119, 1403–1431. [23] Danielsen J. D. and Bishop J. L. (2018) *LPS XLIX*, Abstract #1804. [24] Bishop J. L. and Murad E. (2005) *Am. Mineral.*, 90, 1100–1107. [25] Cloutis E. A. et al. (2006) *Icarus*, 184, 121–157. [26] Bishop J. L. et al. (2013) *Clays Clay Miner.*, 61, 57–74. [27] Bishop J. L. et al. (2008) *Clay Miner.*, 43, 35–54. [28] Bishop J. L. et al. (2002) *Clay Miner.*, 37, 607–616. [29] Benison K. C. and Bowen B. B. (2006) *Icarus*, 183, 225–229. [30] Benison K. C. and Bowen B. B. (2009) *Appl. Geochem.*, 24, 268–284. [31] Clark R. N. et al. (2007) USGS digital spectral library splib06a: U.S. Geological Survey, Digital Data Series 231.